The Dangers of simple usage of Microwave Software

Ulrich L Rohde *, Hans L. Hartnagel **

* Synergy Microwave Corp

201 McLean Blvd. Paterson, NJ, 07504, USA

e-mail: ulr@synergymwave.com

web: www.synergymwave.com:8080/

**Fachgebiet Mikrowellenelektronik, Technische Universitäet Darmstadt,

Merckstr.25, D-64283 Darmstadt, Germany

e-mail: hartnagel@ieee.org

web: www.mwe.tu-darmstadt.de

Introduction:

We have seen many dissertations about the implementation of microwave circuits, where a student has built an oscillator or another circuit, measured it, ran a simulation, obtained different answers and then tried to explain the reasons. Actually there are two main sources of inaccuracy, one being the measurements and the other the simulation. In the case of an oscillator the important parameters are output power, harmonic content and, most important, phase noise.

These three critical parameters are determined under large-signal conditions. Using CAD introduces automatically two weaknesses. The device used for the application needs to be characterized, many times by curve fitting, and needs to match a model of the simulator which itself is mostly an analytical model rather than physics based.

In a simple oscillator case we would like to show that using a rigorous mathematical model the educational benefit outweighs the simplicity of a CAD analysis and subsequent optimization.

The two test cases are a Driscoll oscillator with the crystal resonator in the emitter, which was taken from the literature and the design could have never worked because of errors in the publication data. A CAD tool would not have found the problem but an understanding of the operation allows to find the correction. The next case is the Colpitts oscillator, which offers many choices of design but only the large signal approach will work. This is more analytical rather than trial and error.

This effort is based on using Bessel functions and a calculation in the time and frequency domain. The added benefit is that all physics-based noise models will be used and therefore the student gains much more insight in all the concurrencies. Once the basic set of equations is derived, the first derivative of the feedback components vs. phase noise allows exact optimization.

This type of circuit analysis, which can be applied to many other designs such as amplifiers and mixers, give the best insight into the functionality of circuits in the time domain where we discover such new things like time average loaded Q and noisy feedback or noise-contributing support circuits.

In this paper we will use a simple but in the end highly non-linear circuit, where we will demonstrate the accuracy of our approach using simulations, sets of analytical time domain equations and of course accurate measurements using test equipment from two established manufacturers, Agilent and R&S. Each step of this design provides much better insight in the functionality than the standard teaching approach of this topic resorting to too much CAD. In the following we will show three cases, which will highlight the problems.

Case study of a: Twin T-oscillator using an Infineon BFR93aw, microwave transistor, showing that the linear and the non-linear analysis for the resonant frequency gives a significant different results [1], a analysis of a Driscoll oscillator where the Cad prediction is far too optimistic because it does not have good data for the flicker corner frequency [not provided by the manufacturer] and flicker noise contribution of the crystal and finally the third case is the mathematical analysis of the Colpitts oscillator using the large signal parameter and the Bessel function to get a very close result to both the measured and the CAD simulation [2].

Case 1:

In general and until recently transistor simulations used linear analysis, which turns out to give fairly inaccurate results. To show the base line, here is the example using a RC example. It is based on [1] and operates at 1.6MHz. Figure 1 shows the actual circuit diagram.

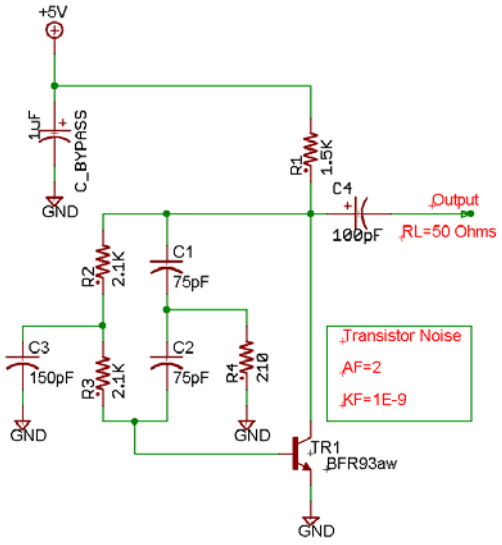

Figure 1: the actual circuit diagrams for 1.6MHz

The literature is full of RC oscillators but very little information is available on its phase noise and the difference between the linear and the non-linear operation. So we analyzed [Figure 1] this oscillator and scaled it to about 1MHz and using a linear simulation determined the following resonance frequency.

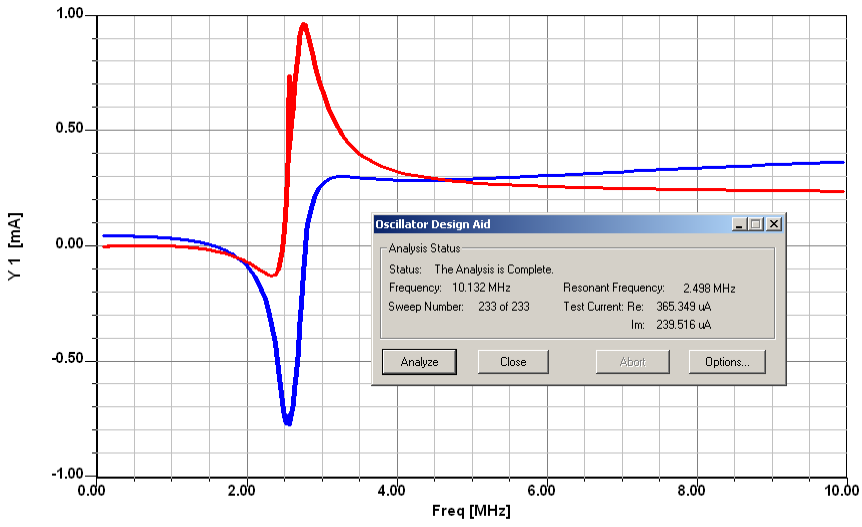

Figure 2: Linear simulation result of the schematic in figure 1.

The linear case indicates the resonance frequency around 2.5GHz. The Y-axis is the RF current in milliamps at the junction between the two resistors, 2.1Kohms and the 150pF capacitors to the ground. This assumes a total linear system and the purpose of this example is to show that the linear simulator can mislead you totally. After this result we used the Ansoft serenade harmonic

balance simulator 8.7V and a validated model for the siemens transistor BFR93aw. The initial DC analysis provides the operating point.

Bias Point Values

Voltage	Current
Vp() = -0.232686 uV	Ip() = 0 A
Vbe(_lib1) = 0.734765 V	Ib(_lib1) = 36.3168 uA
Vce(_lib1) = 0.862989 V	Ic(_lib1) = 2.70409 mA

The results are 2.7mA for 0.86V V_{ce}. The output waveform is slightly distorted and shown in figure 3. Figure 4 shows the harmonic contents. The output frequency as seen in figure 4 is different from the linear prediction and is 1.6MHz. The harmonic suppression is about 14dB. The loaded output terminated into 50 ohms is –19dBm.

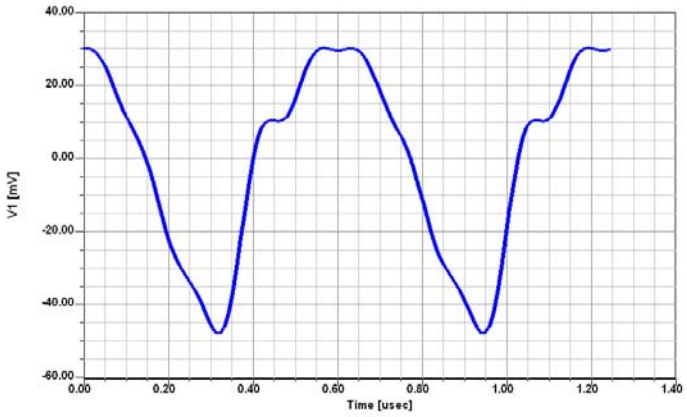

Figure 3: Simulated output waveform.

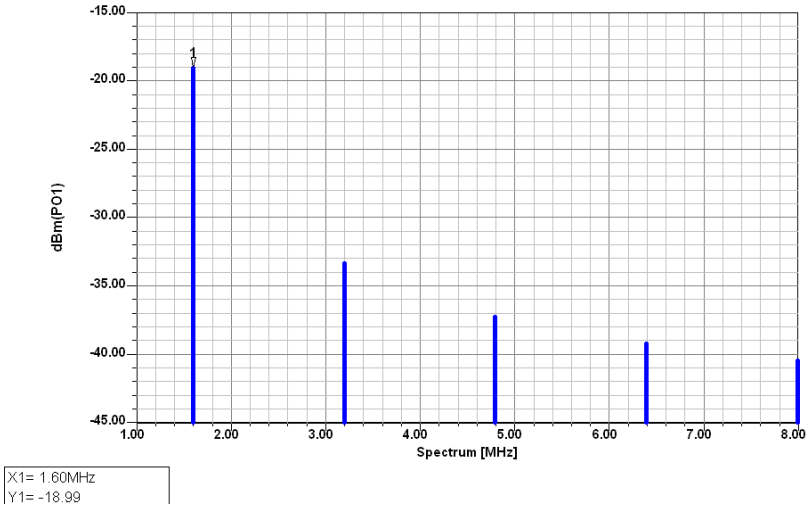

Figure 4: Simulated output power for the schematic in figure 1

We must keep in mind that this is a RC oscillator consisting of a notch filter and does not have a Q in the traditional sense. These types of oscillators typically do not operate into 50 ohms but into some CMOS gates, which are voltage and not power driven. IF we assume that the practical load is 9Kohms then the voltage swing at the output increase to ±900mV, this is 1.8Vp-p at the end to drive the gate.

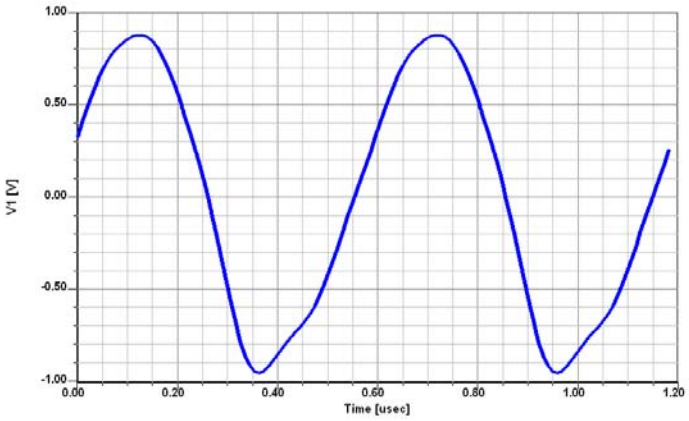

Figure 5: Simulated output waveform with a high impedance termination of 9Kohms.

Now to our surprise the resonant frequency is 1.679MHz a huge difference from the linear approximation. So far we have shown output power harmonic contents and now how about the phase noise.

This information is rarely found in the literature, but here it is shown in figure 6.

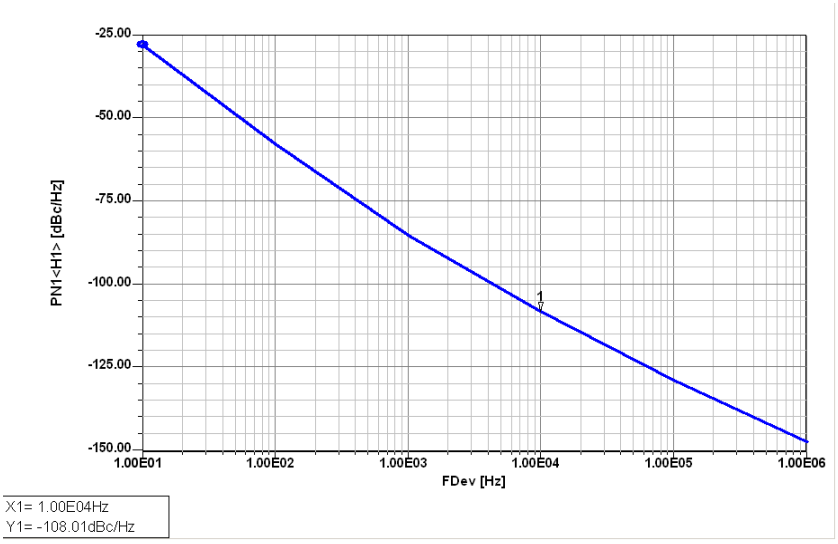

Figure 6: Predicted phase noise in dBc/Hz offset from the carrier frequency ranging from 10Hz to 1MHz of this RC oscillator.

By itself it is not overwhelming but if it is used as a part of the synthesizer loop divided down by the 100 a 40dB improvement, then it looks much better. The 10 KHz offset would be at –148dBc/Hz. It is mixed into a synthesizer it is a good performer.

Again why is this barely found in literature?

1: Most of the CAD tools cannot analyze this accurately. An important test is to validate the existence of the flicker corner frequency. In our case it is at 1 kHz. This is typical for a microwave transistor at this DC current, an audio type transistor or a FET to show much smaller number.

2: Majority of phase noise setups does not operate below 10MHz; Measurements of 5MHz are typically done using a diode multiplier at higher frequency.

Case 2:

One of the promising oscillator is the circuit discover by Driscoll; Its schematic shown in the figure 7.

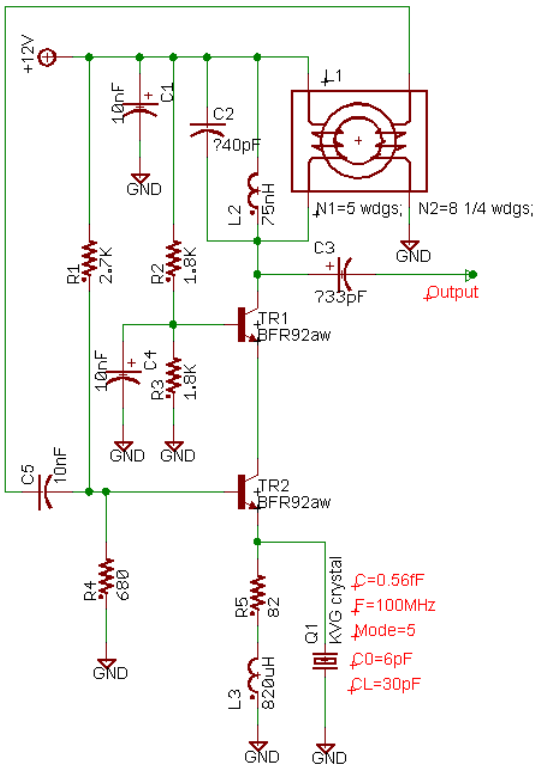

Figure 7: 100MHz crystal oscillator using the Driscoll Schematic.

Essentially it is a cascode amplifier where the output from the second transistor is inverted by 180 degrees and drives the lower transistor. At its resonance frequency the Crystal, grounds the emitter via a small resistor (C of the crystal) and the oscillations starts.

The measured results first. They were obtained using the FSUP.

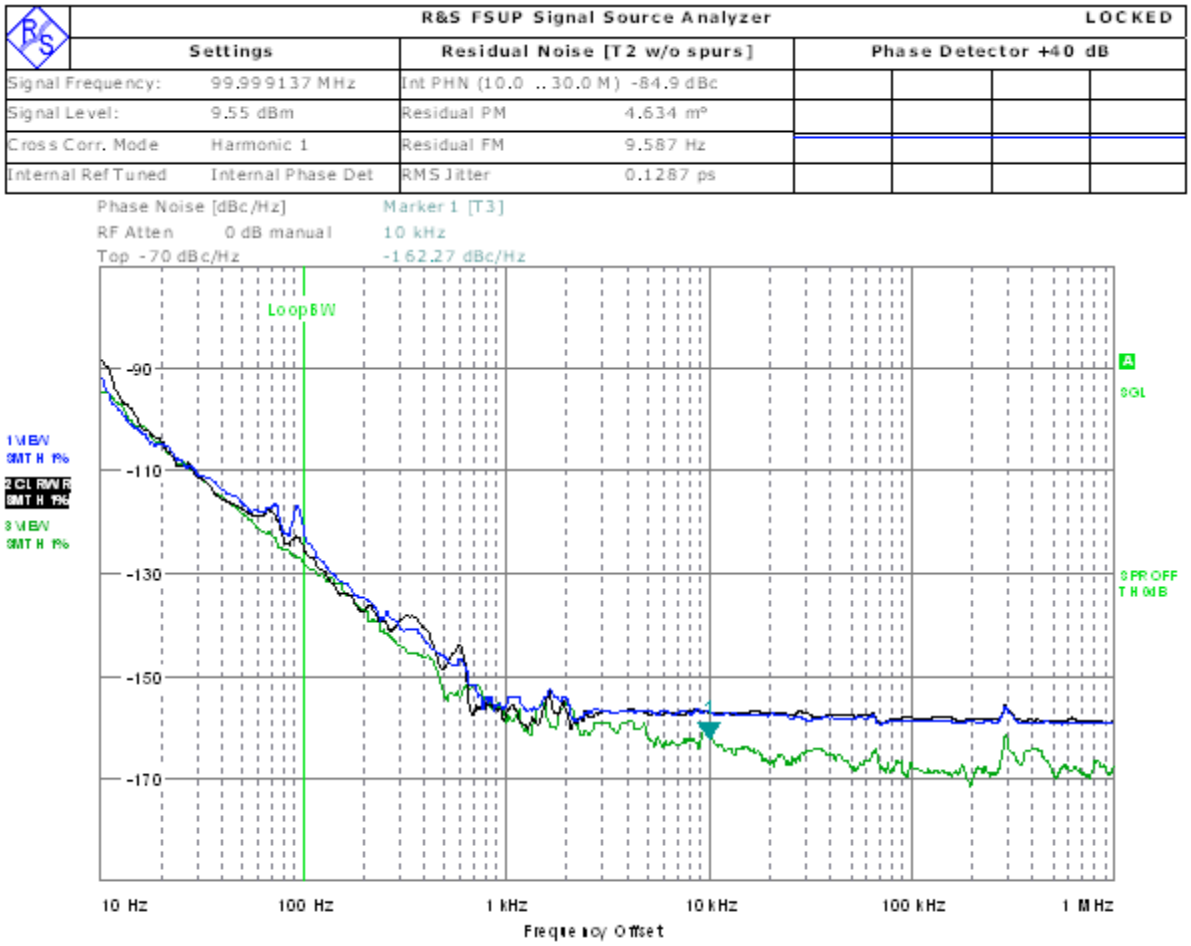

Figure 8: measured result for the 100MHz Crystal oscillator.

The difference between the blue and the green curve is the measurement taken without the buffer (green) and with the buffer amplifier, BGA614, dual Darlington amplifiers (blue curve). We really would like to point out that choice of right buffers is extra ordinarily important and the CAD tools may not give the right answer.

Now let's do the simulation.

The linear simulation tells us 99.998MHz. Because this is a very high Q device and it also maintains its high Q we can expect the circuit simulator to give a similar answer in the nonlinear mode.

The transistor cascode is operated at 17.4mA. The lower transistor TR2, model BFR92aw, has a V_{ce} of 3.46V and the upper transistor TR1 same model has the V_{ce} of 6.94V. The output power is 9.58dBm with the predicted harmonic suppression of 22 dB. The output waveform is shown in the figure 10 and it shows on the upper right corner the harmonic contents.

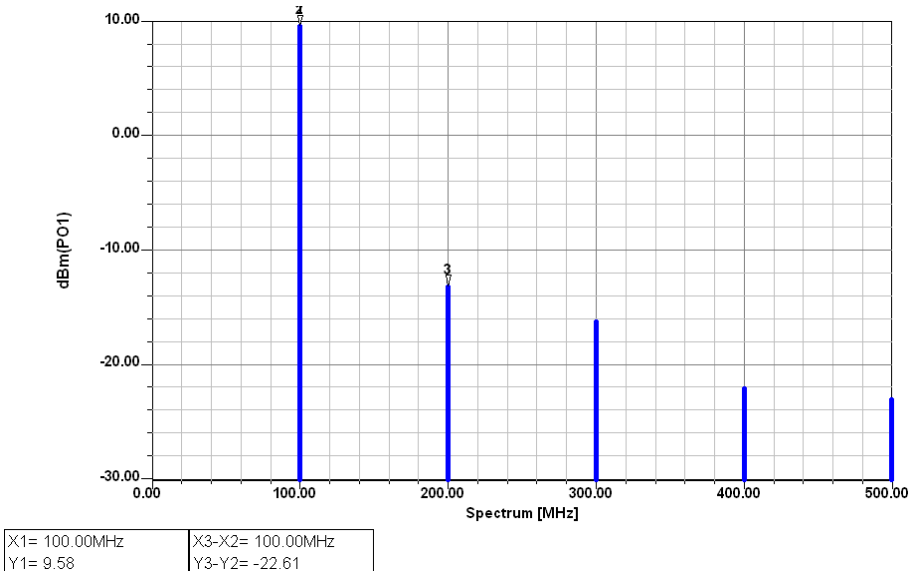

Figure 9 Predicted harmonic contents of the schematic in figure 7.

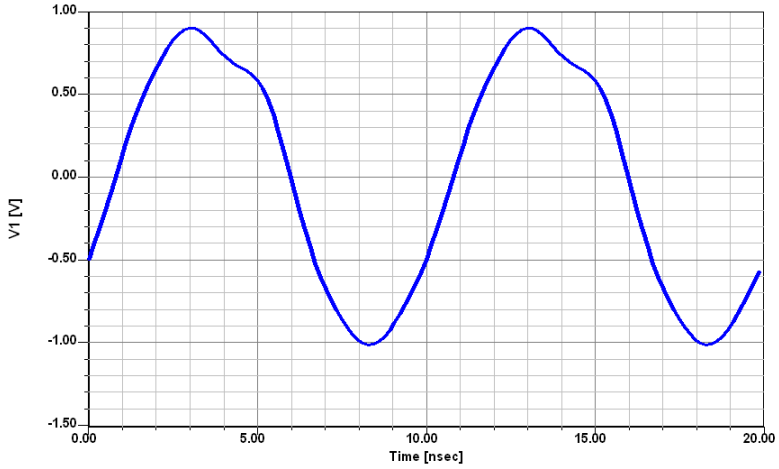

Figure 10: The estimated output waveform for 100MHz crystal oscillator

Now we are curious what the phase noise simulation tells us compared to the measured results.

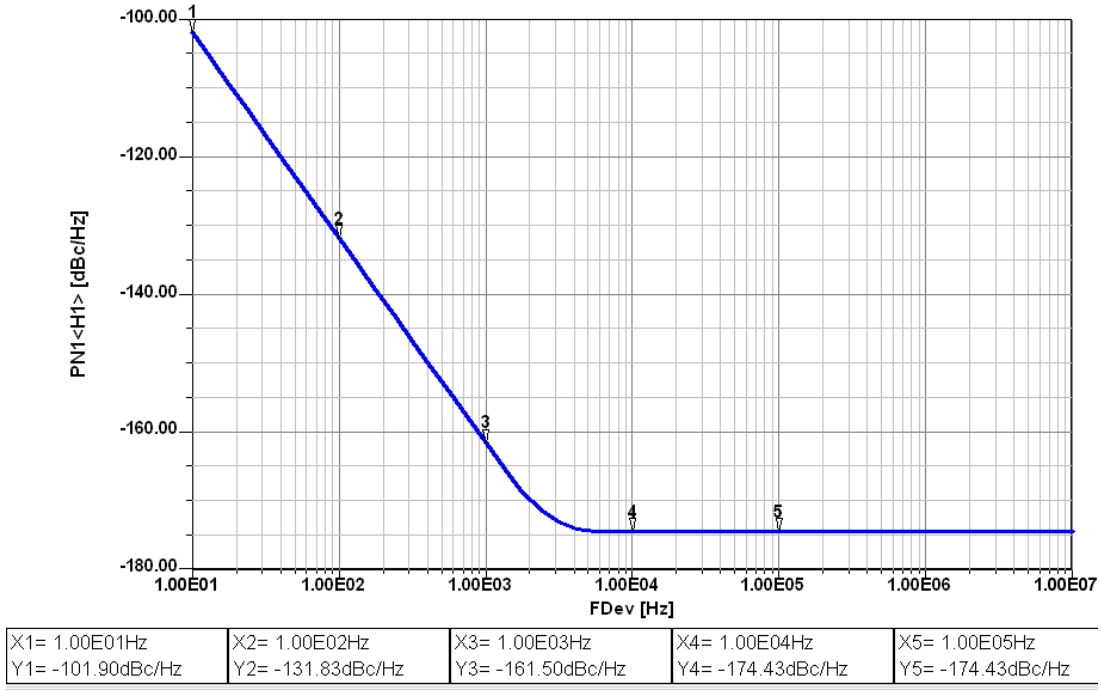

Figure 11: Predicted phase of the 100MHz crystal oscillator from Driscoll.

As we had already anticipated the CAD solution is somewhat erroneous. Since this is a crystal oscillator or a frequency reference it cannot be phase locked easily and there is no easy way to improve it. Here are the results and their deviations.

Frequency offset	10Hz	100Hz	1KHz	10KHz	100Khz
Simulation result	-102dBc	-132dBc	-161.5dBc	-174dBc	-174dBc
Measurement result	-90dBc	-125dBc	-155dBc	-162dBc	-170dBc

Having spent $50,000 for the simulator and $80,000 for the test equipment the simulator is too optimistic. The reason for this lays in the uncertainty of the flicker frequency which none of the manufacturers are willing to give guarantee for, and a type of flicker noise that the crystal has itself. The standard crystal models are not sufficiently accurate for the good modeling.

In case three we like to develop an analytic formula, which greatly eliminates the CAD cost, and its problems and yet gives results were calculations, not simulation agrees with the measurement.

Case 3:

A colpitts oscillator is an attractive oscillator, as it uses the capacitive divider and is essentially an emitter follower, which results in phase shift in transistor much less than a grounded emitter circuit has. For further details on Colpitts oscillator see reference [2].

The colpitts oscillator schematic is as shown below:

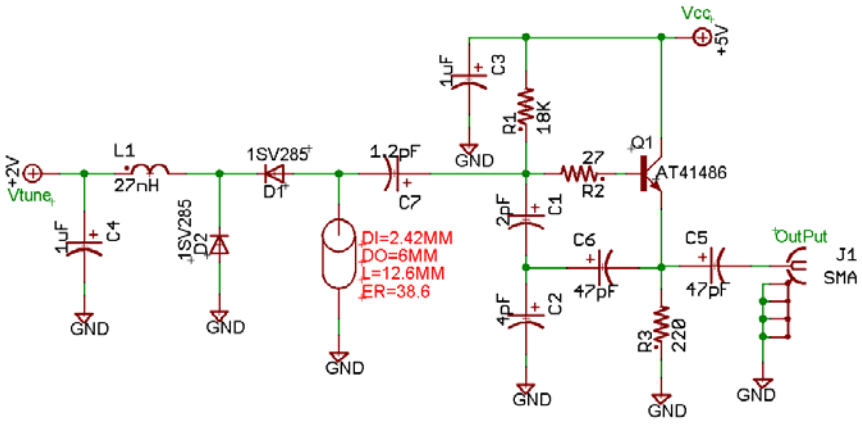

Figure 12: Colpitts oscillator design for 800-900MHz

What we have is a voltage controlled oscillator with Toshiba's 1Sv285 varactor. This fulfills the requirement the author notes for the tuning diodes, page (314) [1]. The simulated results in the book strongly disagree with the simulation [1, page 315 figure 7.19]

Frequency offset	100Hz	1KHz	10KHz	100Khz	1Mhz
Simulation result with diode	-22dBc	-52dBc	-82dBc	-111dBc	-136dBc
Simulation result without diode	-51.5dBc	-81dBc	-110dBc	-137dBc	-158dBc

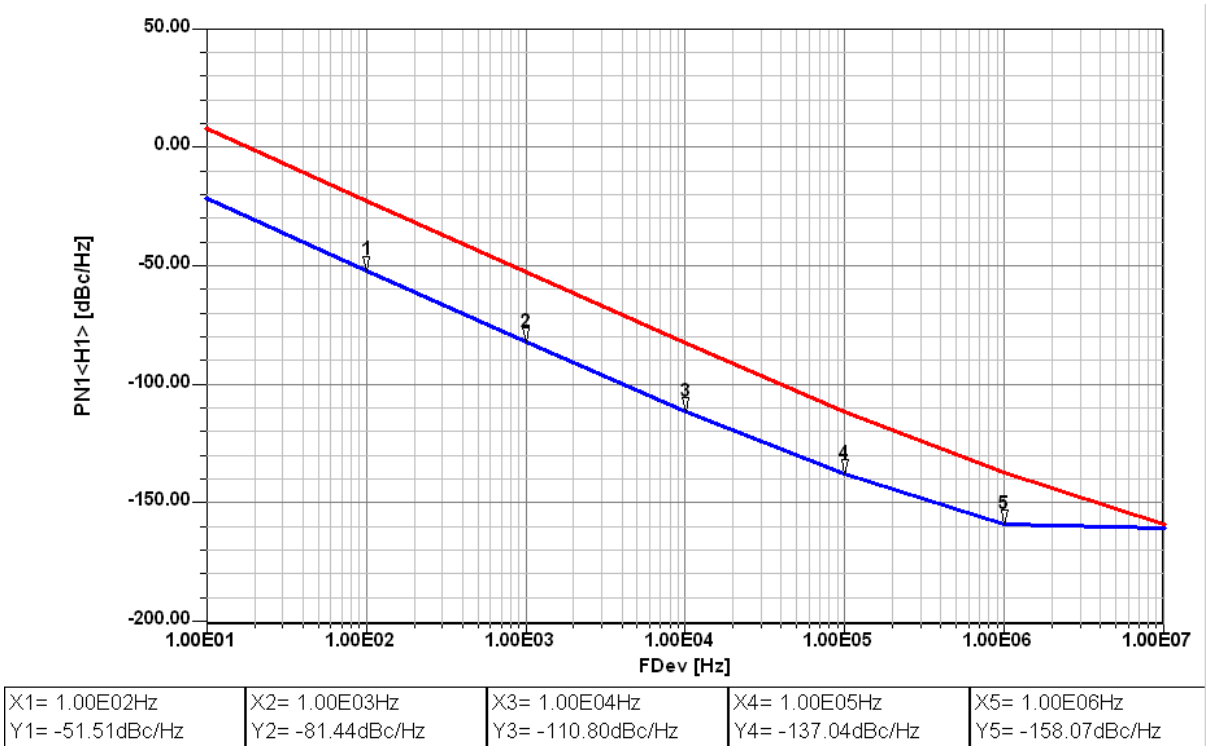

Figure 13: Predicted phase noise of the schematic in figure 12. The blue curve is with fixed capacitors, and the red curve is the phase noise with diodes.

As stated in the beginning a correct analysis of the oscillator, which is a transistor operating in the large signal stage, requires large signal parameters. The amplifier circuit applies enough negative feedback, to compensate the losses of the tuned circuit and the parasitic elements. Figure 14 shows the typical block diagram of conventional feedback oscillator circuit.

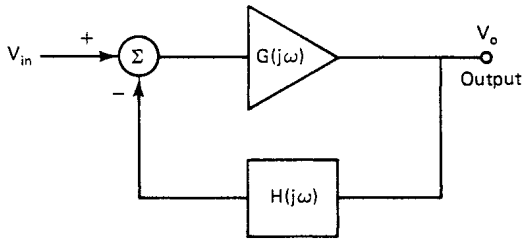

Figure14: A typical block diagram of feedback oscillator circuit [2]

Barkausen in 1935 was the first to state that for this case the product of forward voltage gain and the feedback voltage gain had to be > 1.

$$\frac{V_o}{V_{in}} = \frac{\mu}{1-\mu\beta} > 1 \qquad (1)$$

In recent years engineers used a linear approach and stipulated that the positive loss resistance and to be compensated by a parallel or series negative resistance.

Figure 15 shows a Colpitts oscillator, its input impedance with the feedback capacitors C1 and C2 connected, is calculated and to be seen later.

In the practical case, the device parasitics and loss resistance of the resonator will play an important role in the oscillator design. Figure 15 incorporates the base lead-inductance L_p and the package-capacitance C_p.

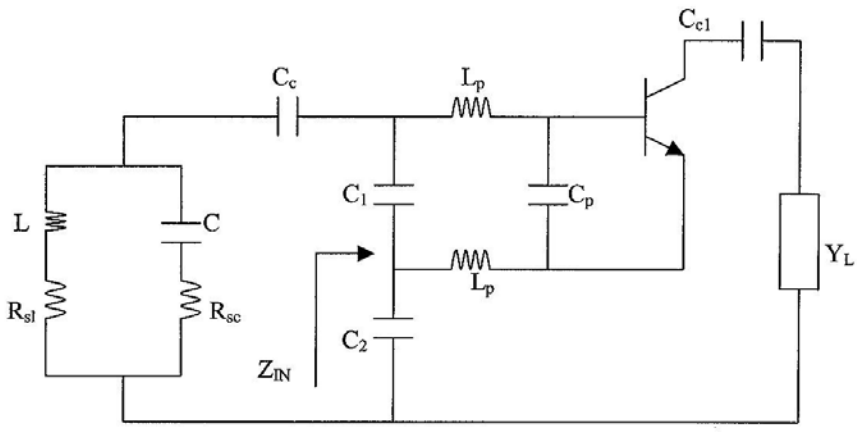

Figure 15: Colpitts oscillator with base-lead inductances and package capacitance. C_C is neglected.

The expression of input impedance is given as [2]

$$Z_{IN}\big|_{pacakage} = -\left[\frac{Y_{21}}{\omega^2(C_1+C_p)C_2}\frac{1}{(1+\omega^2 Y_{21}^2 L_p^2)}\right] - j\left[\frac{(C_1+C_P+C_2)}{\omega(C_1+C_P)C_2} - \frac{\omega Y_{21} L_P}{(1+\omega^2 Y_{21}^2 L_p^2)}\frac{Y_{21}}{\omega(C_1+C_P)C_2}\right] \quad (2)$$

$$Z_{IN}\big|_{without-pacakage} = -\left[\frac{Y_{21}}{\omega^2 C_1 C_2}\right] - j\left[\frac{(C_1+C_2)}{\omega C_1 C_2}\right] \quad (3)$$

Where L_p is the base-lead inductance of the bipolar transistor and C_p is base-emitter package capacitance. All further circuits are based on this model. From the expression above, it is obvious that the base lead-inductance makes the input capacitance appear larger and the negative resistance appears smaller.

The equivalent negative resistance and capacitance can be defined as [2]

$$R_{NEQ} = \frac{R_N}{(1+\omega^2 Y_{21}^2 L_p^2)} \qquad (4)$$

The assumptions in the past were if R_{NEQ} was sufficiently negative then stable oscillation occurs. However the oscillator is inherently a linearized non-linear circuit and the assumption that this R_{NEQ} was sufficient was not always correct.

The value of R_{NEQ} is the starting value before oscillation, and as the large signal condition takes over, Y21 decreases!

This large signal effect will be analyzed and will become part of the noise analysis und large signal condition.

Large Signal Analysis:

In order to better understand the noise generation in an oscillator, we need to first leave the traditional small signal analysis and consider the actual large signals conditions. So instead of using the familiar linear S parameter, we now resort to their large signal equivalent,

Large Signal *S*-Parameter Measurements

Assume S_{11} and S_{21} are functions only of incident power at port 1 and S_{22} and S_{12} are functions only of incident power at port 2. Note: the plus (+) sign indicates the forward wave (voltage) and the minus (-) sign would be the reflected wave (voltage).

$$S_{11} = S_{11}\left(\left|V_1^+\right|\right) \quad S_{12} = S_{12}\left(\left|V_2^+\right|\right) \qquad (5)$$

$$S_{21} = S_{21}\left(\left|V_1^+\right|\right) \quad S_{22} = S_{22}\left(\left|V_2^+\right|\right) \qquad (6)$$

The relationship between the traveling waves now becomes

$$V_1^- = S_{11}(V_1^+)V_1^+ + S_{12}(V_2^+)V_2^+ \qquad (7)$$

$$V_2^- = S_{21}(V_1^+)V_1^+ + S_{22}(V_2^+)V_2^+ \qquad (8)$$

Measurement is possible if V_1^+ is set to zero,

$$S_{12}(V_2^+) = \frac{V_1^-(V_2^+)}{V_2^+} \qquad (9)$$

Check the assumption by simultaneous application of V_1^+ and V_2^+

$$\begin{bmatrix} V_1^- \\ V_2^- \end{bmatrix} = \begin{bmatrix} F_1(V_1^+, V_2^+) \\ F_2(V_1^+, V_2^+) \end{bmatrix} \qquad (10)$$

If harmonics are neglected, a general decomposition is

$$\begin{bmatrix} V_1^-(V_1^+, V_2^+) \\ V_2^-(V_1^+, V_2^+) \end{bmatrix} = \begin{bmatrix} S_{11}(V_1^+, V_2^+) & S_{12}(V_1^+, V_2^+) \\ S_{21}(V_1^+, V_2^+) & S_{22}(V_1^+, V_2^+) \end{bmatrix} \begin{bmatrix} V_1^+ \\ V_2^+ \end{bmatrix} \qquad (11)$$

Figure 16 shows the R&S vector analyzer and the test fixture for the transistor of choice.

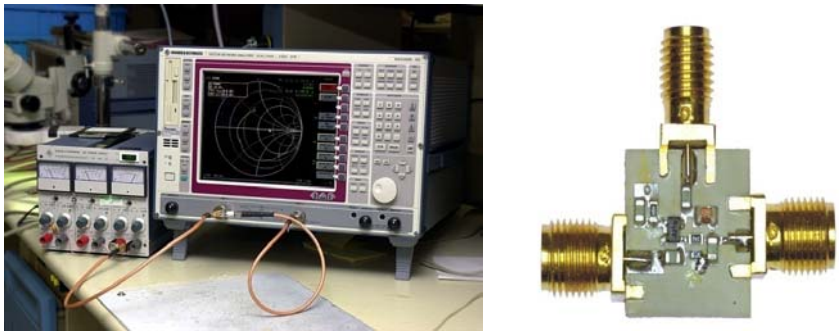

Figure 16: Typical measurement setup for evaluation of large signal parameters (R&S vector analyzer and the test fixture for the transistor of choice)

The bias, drive level, and frequency dependent S parameters are then obtained for practical use. Since we did not have an access to AT41486, we used the infineon transistor BFP520 as an example.

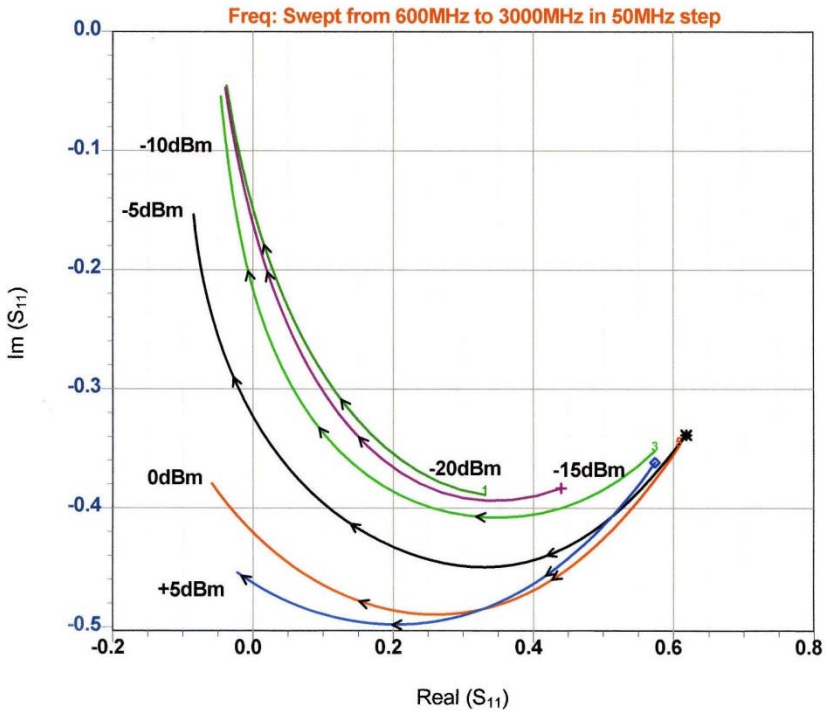

Figure 17: Measured large-signal S_{11} of the BFP520 [2, pp. 68].

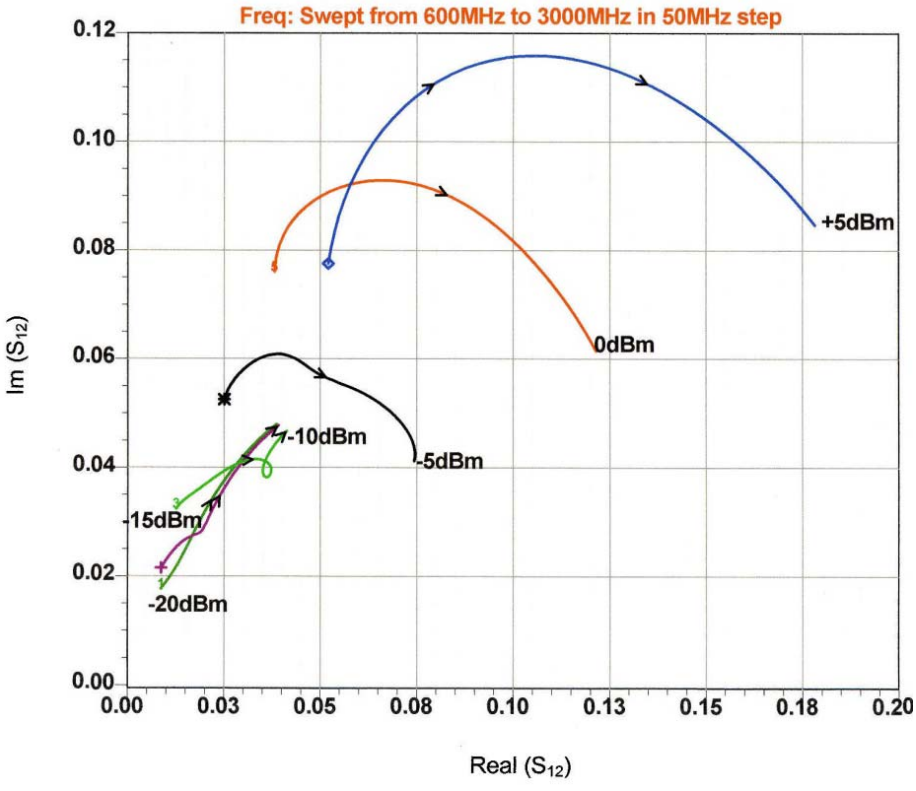

Figure 18: Measured large-signal S_{12} of the BFP520 [2, pp. 68]

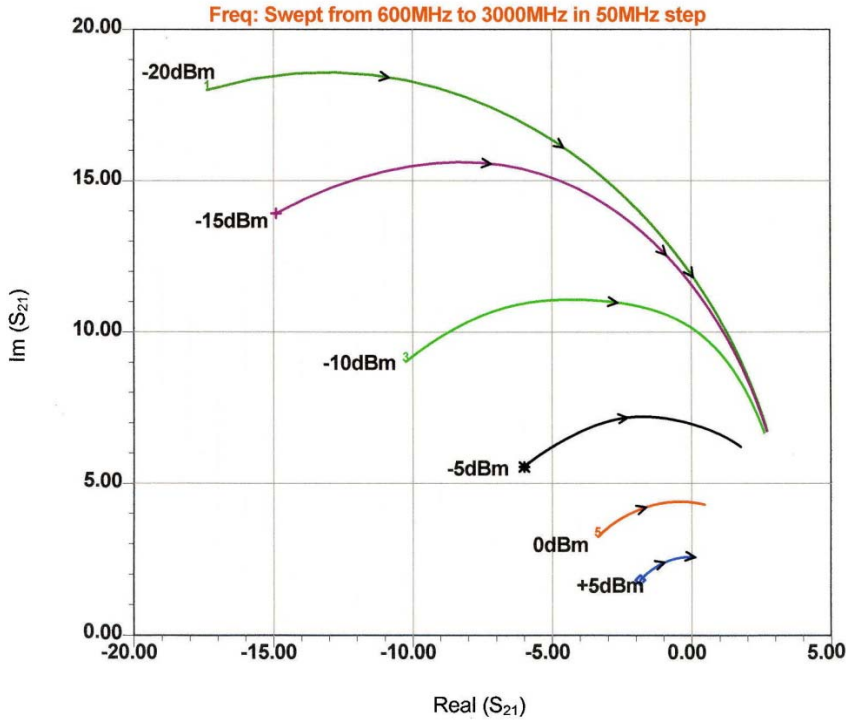

Figure 19: Measured large-signal S_{21} of the BFP520 [2, pp. 69].

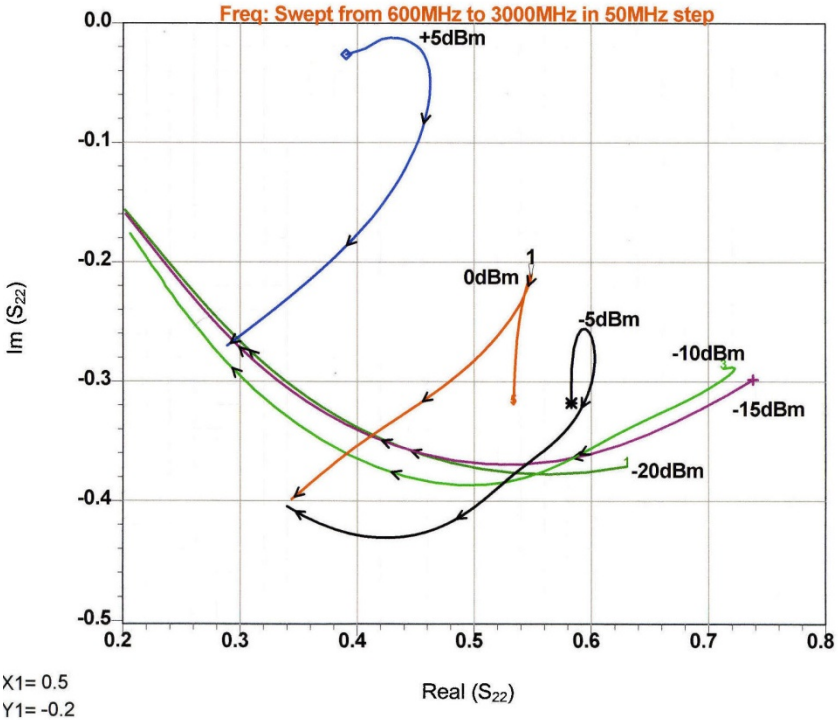

Figure 20: Measured large-signal S_{22} of the BFP520 [2, pp. 69].

The legal definitions of large signal S parameter apply only for a 50-Ohm termination. In our case, an oscillator, the harmonic related S parameters could be neglected. Otherwise the load pull technique applies.

Why are these parameters of interest for us?

They show the dramatic change of S_{11} and S_{21} as a function of frequency and bias level. For the Colpitts oscillator, where the collector is separated S22 is less relevant and since the feedback is external, S12 also less important, depending on the frequency. If calculating the negative resistance to compensate the losses, we must insert the large signal frequency depending value for Y_{21}.

Large-Signal Oscillator Design and Start-Up Condition

As a basic requirement for producing a self-sustained near-sinusoidal oscillation, an oscillator must have a pair of complex-conjugate poles on the imaginary axis i.e. in the right half of s-plane with α>0.

$$P(p_1, p_2) = \alpha \pm j\beta \qquad (12)$$

When the *Barkhausen criterion* is met, the two conjugate poles of the overall transfer function are located on the imaginary axis of the s-plane. Any departure from that position will lead to an increase or a decrease of the amplitude of the oscillator output signal in time domain, which is shown in Figure 21. Figure 22 shows the typical transient simulation of a ceramic resonator-based high-Q oscillator, where node of the voltage is taken from the emitter.

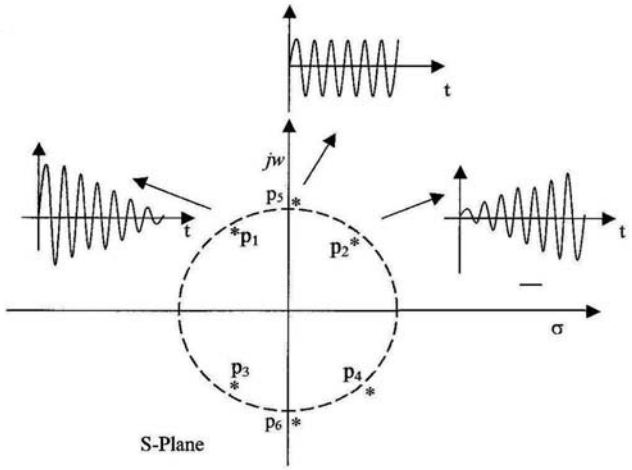

Figure 21: Typical frequency domain root locus and the corresponding time domain response [2, pp. 96].

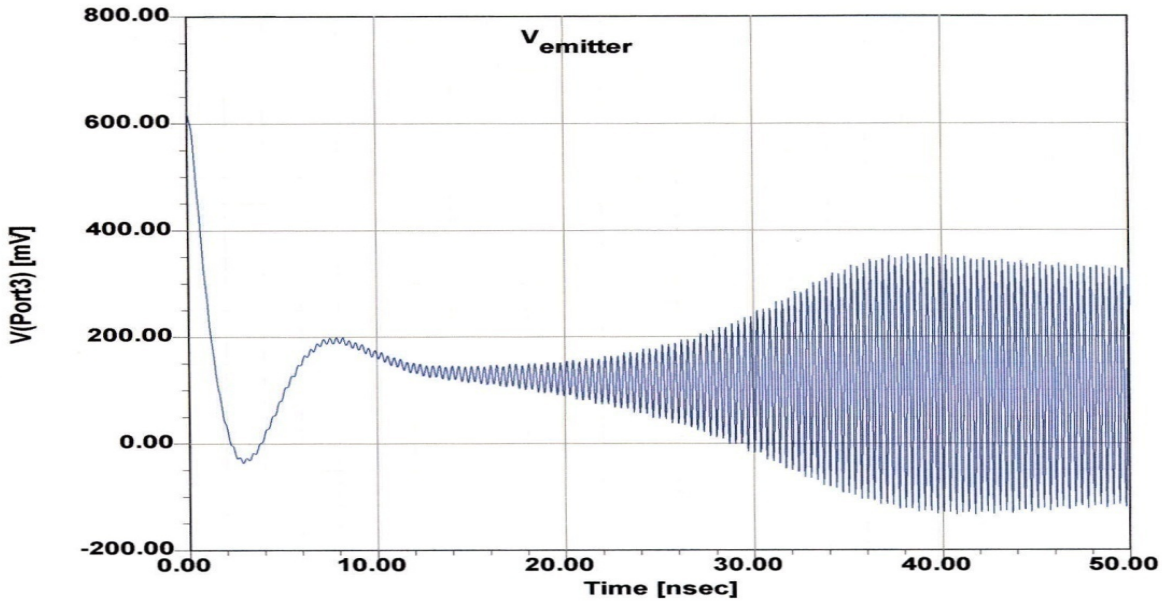

Figure 22: Typical transient simulation of a ceramic resonator-based high-Q oscillator (node of the voltage for display is taken from the emitter) [2, pp.100].

The steady state oscillation condition can be expressed as

$$\Gamma_a(A, f)\Gamma_r(f)\big|_{f=f_0} \Rightarrow \Gamma_a(A_0, f_0)\Gamma_r(f_0) = 1 \qquad (13)$$

For brief insights about the negative resistance oscillator, a block diagram of one-port negative reflection model is shown in Figure 23.

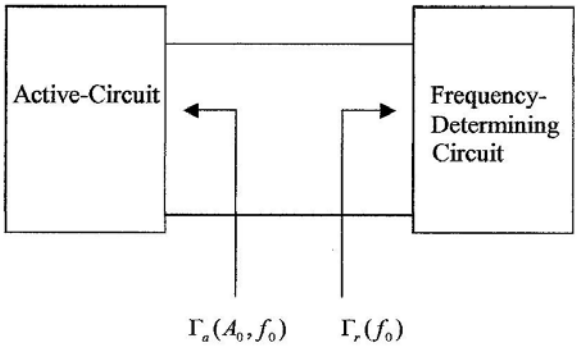

Figure 23: Schematic diagram of a one-port negative reflection model.

Figure 24 illustrates the start and steady-state oscillation conditions.

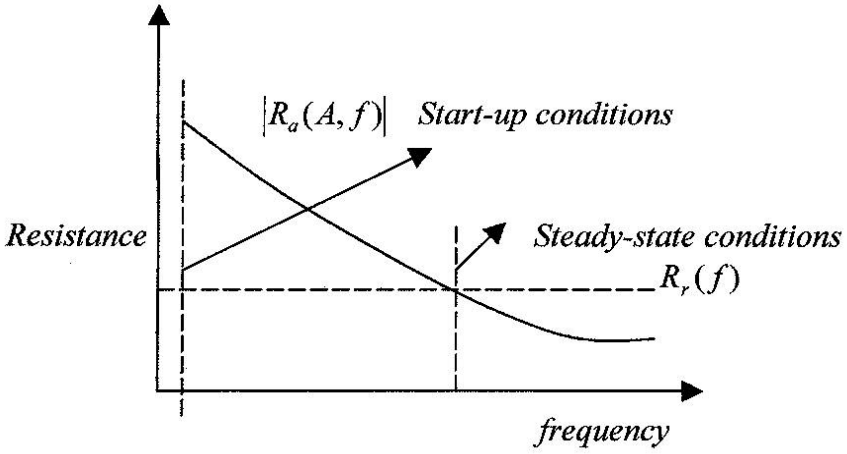

Figure 24: A typical start and steady-state oscillation conditions.

As described in Figure 24, R_a (*A*, *f*) is the starting negative Resistance, which gets lower as the amplitude increases. Therefore, feedback must be sufficient to maintain enough negative resistance to sustain oscillating.

Time-Domain Behavior

The large-signal transfer characteristic affecting the current and voltage of an active device in an oscillator circuit is nonlinear. It limits the amplitude of the oscillation and produces harmonic content in the output signal. The resonant circuit and resulting phase shift sets the oscillation frequency. The nonlinear, exponential relationship between the voltage and current of a bipolar transistor is given as

$$i(t) = I_s e^{\frac{qv(t)}{kT}} \tag{14}$$

$$v(t) = V_{dc} + V_1 \cos(wt) \tag{15}$$

$$i_e(t) = I_s e^{\frac{qv(t)}{kT}} \tag{16}$$

$$i_e(t) = I_s e^{\frac{qV_{dc}}{kT}} e^{\frac{qV_1 \cos(wt)}{kT}} \tag{17}$$

$$i_e(t) = I_s e^{\frac{qV_{dc}}{kT}} e^{x\cos(wt)} \tag{18}$$

assuming, $I_c \approx I_e$ (β>10)

The normalized drive level is

$$x = \frac{V_1}{(kT/q)} = \frac{qV_1}{kT} \qquad (19)$$

$i_e(t)$ is the emitter current and x is the drive level which is normalized to kT/q.

From the Fourier series expansion, $e^{x\cos(wt)}$ is expressed as

$$e^{x\cos(wt)} = \sum_n a_n(x)\cos(nwt) \qquad (20)$$

$a_n(x)$ is a Fourier coefficient and given as

$$a_0(x)\big|_{n=0} = \frac{1}{2\pi}\int_0^{2\pi} e^{x\cos(wt)}d(wt) = I_0(x) \qquad (21)$$

$$a_n(x)\big|_{n>0} = \frac{1}{2\pi}\int_0^{2\pi} e^{x\cos(wt)}\cos(nwt)d(wt) = I_n(x) \qquad (22)$$

$$e^{x\cos(wt)} = \sum_n a_n(x)\cos(nwt) = I_0(x) + \sum_1^{\infty} I_n(x)\cos(nwt) \qquad (23)$$

$I_n(x)$ is the modified Bessel function.

As $x \to 0 \Rightarrow I_n(x) \to \frac{(x/2)^n}{n!}$ (24)

$I_0(x)$ are monotonic functions having positive values for x≥0 and n≥0; $I_0(0)$ is unity, whereas all higher order functions start at zero.

The short current pulses are generated from the growing large-signal drive level across the base-emitter junction, which leads to strong harmonic generation. The emitter current represented above can be expressed in terms of harmonics as [2].

$$i_e(t) = I_s e^{\frac{qV_{dc}}{kT}} I_0(x)\left[1 + 2\sum_1^{\infty}\frac{I_n(x)}{I_0(x)}\cos(nwt)\right] \qquad (25)$$

$$I_{dc} = I_s e^{\frac{qV_{dc}}{kT}} I_0(x) \tag{26}$$

$$V_{dc} = \frac{kT}{q}\ln\left[\frac{I_{dc}}{I_s I_0(x)}\right] \Rightarrow \frac{kT}{q}\ln\left[\frac{I_{dc}}{I_s}\right] + \frac{kT}{q}\ln\left[\frac{1}{I_0(x)}\right] \tag{27}$$

I_s = collector saturation current

$$V_{dc} = V_{dcQ} - \frac{kT}{q}\ln I_0(x) \tag{28}$$

$$i_e(t) = I_{dc}\left[1 + 2\sum_1^{\infty}\frac{I_n(x)}{I_0(x)}\cos(nwt)\right] \tag{29}$$

αI_e and Y_{21} are the current source and large-signal transconductance of the device given by the ratio of the fundamental-frequency component of the current to the fundamental-frequency of the drive voltage.

$$Y_{21} = \left.\frac{I_{1peak}}{V_{1peak}}\right|_{fundamental-frequency} \tag{30}$$

$$I_1\big|_{n=1} = I_{dc}\left[1 + 2\sum_1^{\infty}\frac{I_1(x)}{I_0(x)}\cos(wt)\right] \Rightarrow I_{1peak} = 2I_{dc}\frac{I_1(x)}{I_0(x)} \tag{31}$$

x = normalized drive level

$$V_1\big|_{peak} = \frac{kT}{q}x \tag{32}$$

$$Y_{21}\big|_{large-signal} = G_m(x) \tag{33}$$

$$Y_{21}\big|_{small-signal} = \left.\frac{I_{dc}}{kT/q}\right| = g_m \tag{34}$$

$$Y_{21}\big|_{large-signal} = G_m(x) = \frac{qI_{dc}}{kTx}\left[\frac{2I_1(x)}{I_0(x)}\right]_{n=1} = \frac{g_m}{x}\left[\frac{2I_1(x)}{I_0(x)}\right]_{n=1} \tag{35}$$

$$\frac{[Y_{21}\big|_{large-signal}]_{n=1}}{[Y_{21}\big|_{small-signal}]_{n=1}} = \frac{G_m(x)}{g_m} \Rightarrow \frac{2I_1(x)}{xI_0(x)} \tag{36}$$

$$|Y_{21}|_{small-signal} > |Y_{21}|_{large-signal} \Rightarrow g_m > G_m(x) \qquad (37)$$

This allows us to calculate the frequency dependent transconductance, which is needed to optimize the circuit for best noise performance.

The following picture (Figure 25) shows the collector current as a function of time and the normalized base drive voltage *x*. For larger values of *x*, the current and voltage peaks may require a larger transistor. As a result, the time the tuned circuit during less time gets loaded, is reduced and the time average Q is higher.

Figure 26 shows the phase noise of an LC-based 1GHz oscillator as a function of X. For higher values of X the phase noise improves significantly.

The dependency of x can be expressed as

$$x = \frac{R_P G_m C_2}{C_1} \qquad (38)$$

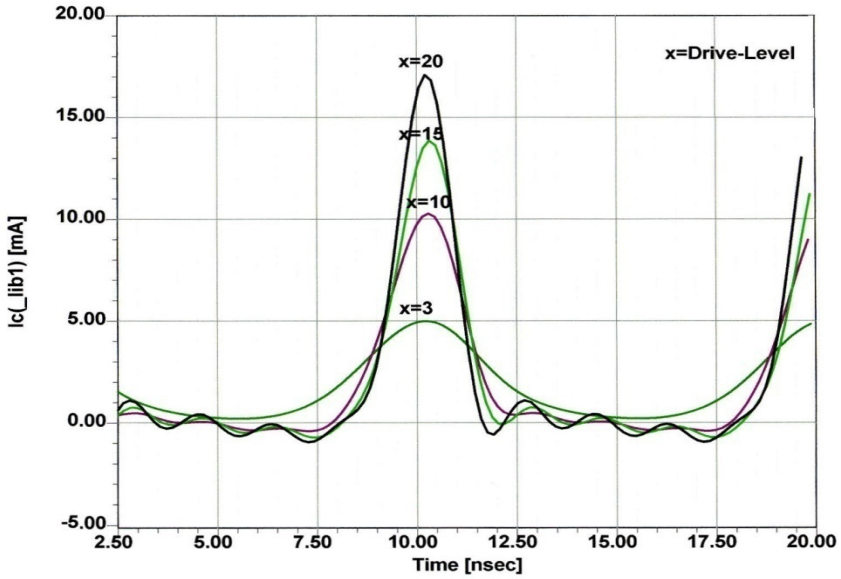

Figure 25: Plot shows the collector current as a function of time with respect to normalized base drive Voltage *x*.

For large drive level, $x \propto C_2$, and the corresponding conduction angle of the output current is given as

$$\varphi = \cos^{-1}\left[1 + \frac{\ln(0.05)}{x}\right] \Rightarrow \varphi \approx \cos^{-1}\left[1 - \frac{3}{x}\right] \qquad (39)$$

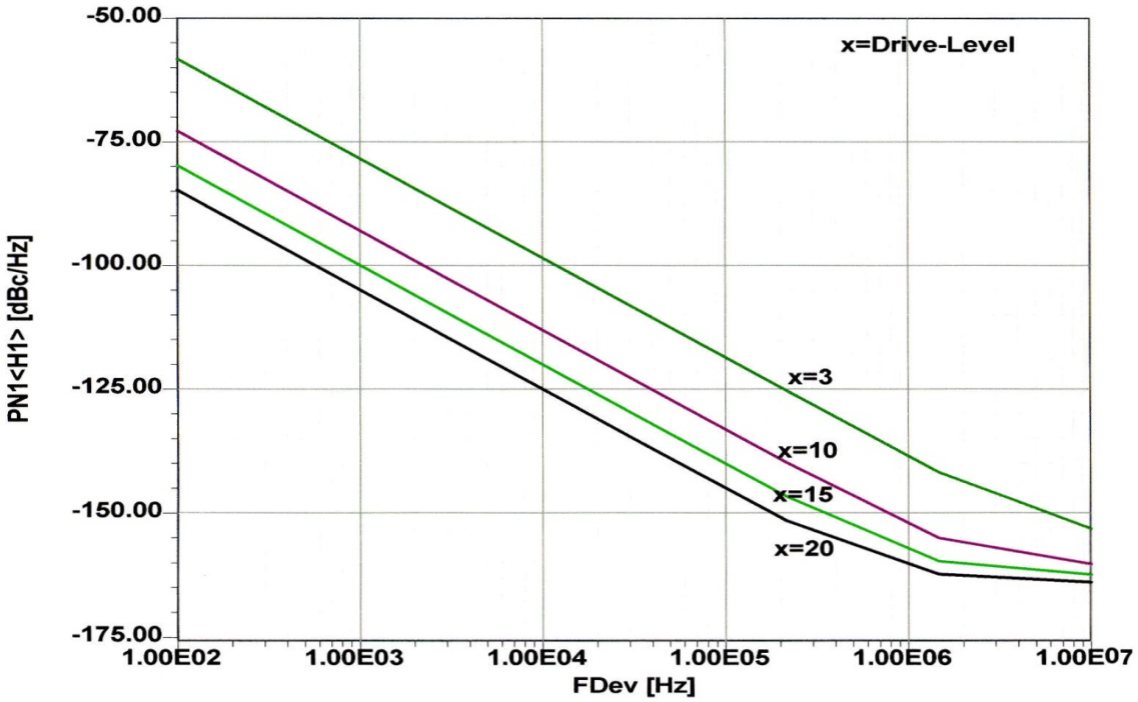

Figure 26: A typical phase noise plot of 1GHz oscillator as a function of x

There is a limit for x, not only due to the limits of voltage and current but also because of reverse biasing of the base collector diode which then makes the circuit really noisy.

Having learned how to design the feedback circuit and introduced the conducting angle and its calculation we have simulated and confirmed the influence on the phase noise, but have not really introduced the oscillator phase noise.

Phase noise in Oscillators

A Linear approach:

In 1965 Leeson developed a model for a noisy transistor oscillator based on a phase modulator, an amplifier, a low pass filter and a resonator, see (Figure 27). In general, oscillator can be viewed as a mixer, where the sum of all inputs is collected and superimposed on the oscillator. Figure 28 shows the components where oscillator acts like a mixer circuit.

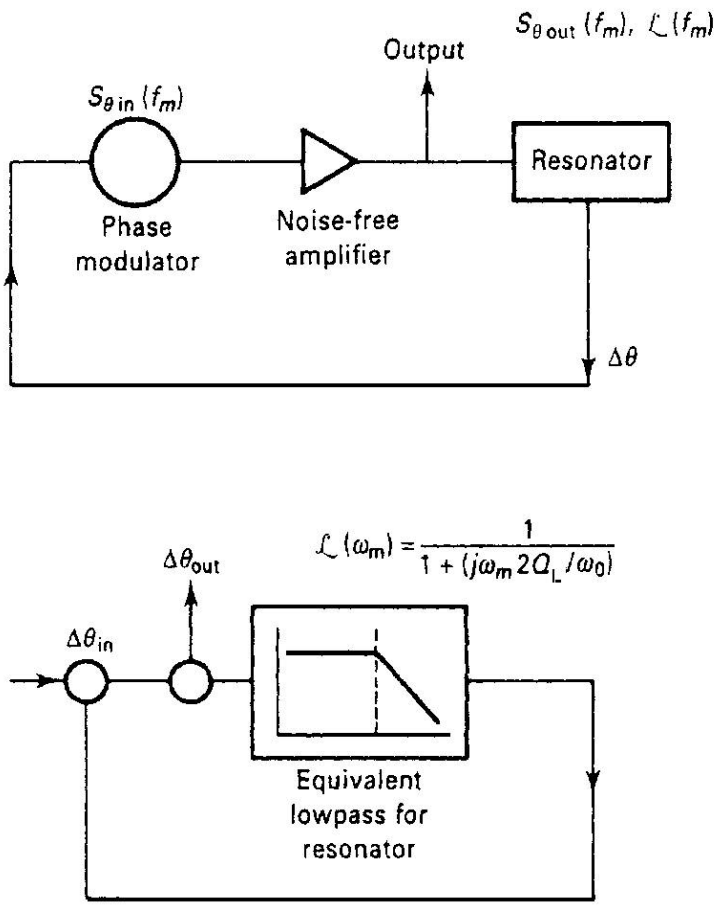

Figure 27: A typical linear oscillator phase noise model (block diagram)

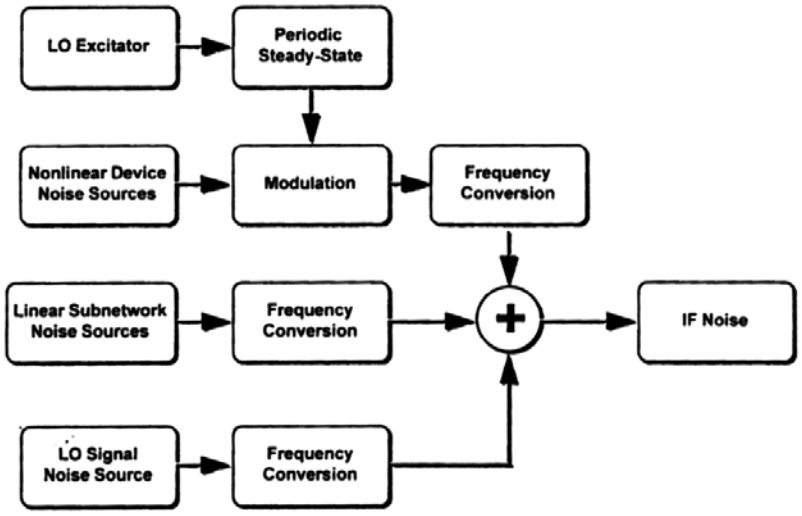

Figure 28: A typical block diagram of mixer circuit, where the oscillator acts like a mixer.

From [2], the resulting signal in linear terms can be calculated as

$$\mathcal{L}(f_m) = \frac{1}{2}\left[1 + \frac{\omega_o^2}{4\omega_m^2}\left(\frac{P_{\text{in}}}{\omega_o W_e} + \frac{1}{Q_{\text{unl}}} + \frac{P_{\text{sig}}}{\omega_o W_e}\right)^2\right]\left(1 + \frac{\omega_c}{\omega_m}\right)\frac{FkT_o}{P_{\text{sav}}}$$

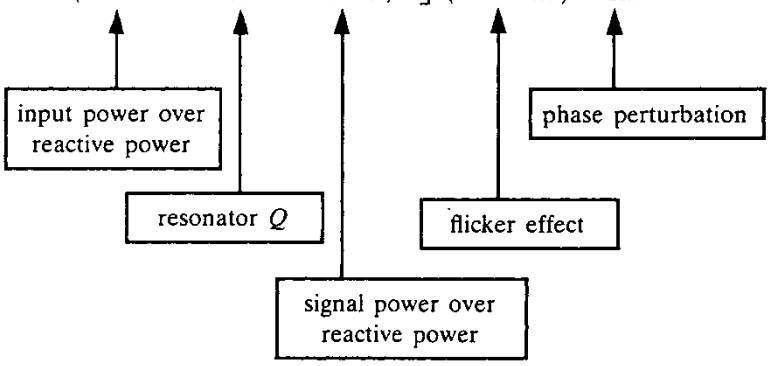

(40)

Equation (40) is the linear Leeson equation, with the pushing effect omitted and the flicker term added by Dieter Scherer (Hewlett Packard, about 1975), the final version with the pushing (VCO effect) added by Rohde, is

$$L\ (f_m) = 10\log\left\{\left[1 + \frac{f_0^{\,2}}{(2f_m Q_L)^2}\right]\left(1 + \frac{f_c}{f_m}\right)\frac{FkT}{2P_{sav}} + \frac{2kTRK_0^{\,2}}{f_m^{\,2}}\right\} \qquad (41)$$

Where

$L\ (f_m)$ = ratio of sideband power in a 1 Hz bandwidth at f_m to total power in dB

f_m = frequency offset

f_0 = center frequency

f_c = flicker frequency

Q_L = loaded Q of the tuned circuit

F = noise factor

$kT = 4.1 \times 10^{-21}$ at 300 K_0 (room temperature)

P_{sav} = average power at oscillator output

R = equivalent noise resistance of tuning diode (typically 50 Ω - 10 kΩ)

K_o = oscillator voltage gain

The problem with this is that key values like loaded Q, large signal NF and output power are not known a priory and the effect of transistor distortion are not included. In some way this provides sometimes an unrealistic good phase noise. On the other hand, it shows the limitation for reasonable values and this presentation will show some mechanism to overcome this.

Figure 29 shows the plot for an ideal 1 GHz LC-based oscillator phase noise of about -140dBc/Hz at offset of 10 kHz offset, assuming unloaded Q of 1E6, loaded Q of 500, noise factor 6 dB, flicker frequency 1kHz, oscillator voltage gain 1Hz/V, equivalent noise resistance of tuning diode 1Ohm and average power at oscillator output 10dBm. Even today this is very much state of the art designer can achieve.

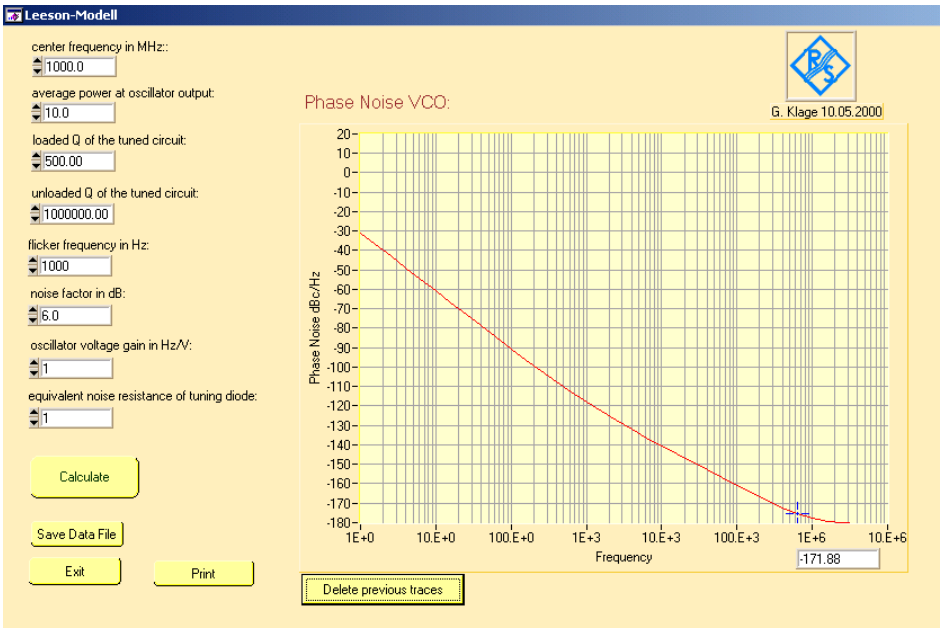

Figure 29: A typical phase noise plot for an ideal 1 GHz oscillator phase noise of about –140dBc/Hz at offset of 10 kHz offset, assuming unloaded Q of 1E6, loaded Q of 500, noise factor 6 dB, flicker frequency 1kHz, oscillator voltage gain 1Hz/V, equivalent noise resistance of tuning diode 1Ohm and average power at oscillator output 10dBm.

The non-linear noise approach [2, Ch-8]:

The equations (41) use a linearized system and are too simplified.

To start the nonlinear noise calculation, we look at the noise sources. The resonator noise is [2, Ch-8, pp. 159-232]

$$\left|\overline{e_R^2(f)}\right|_{\omega=\omega_0} = 4kTBR_s \qquad (42)$$

R_s is the series equivalent noise resistance, based on the losses of the resonator.

The circuit equation for the oscillator with the negative resistance present is [2, Ch-8, pp. 159-232]

$$L\frac{di(t)}{dt}+(R_L-R_N(t))i(t)+\frac{1}{C'}\int i(t)dt=e_N(t) \qquad (43)$$

This is a non-homogeneous differential equation, which can be simplified to [2, Ch-8, pp. 159-232]

$$L\left[-I_1(t)(\omega+\frac{d\varphi_1(t)}{dt})\sin[\omega t+\varphi_1(t)]+\frac{dI_1(t)}{dt}\cos[\omega t+\varphi_1(t)]\right]+\left[(R_L-R_N(t))I(t)\right]+$$

$$\frac{1}{C}\left\{\left[\frac{I_1(t)}{\omega}-\frac{I_1(t)}{\omega^2}\left(\frac{d\varphi_1(t)}{dt}\right)\right]\sin[\omega t+\varphi_1(t)]+\frac{1}{\omega^2}\left(\frac{dI_1(t)}{dt}\right)\cos[\omega t+\varphi_1(t)]\right\}=e_N(t) \qquad (44)$$

Further

where $\overline{R_N(t)}$ is the average negative resistance under large signal condition.

$$\overline{R_N(t)}=\left[\frac{2}{T_0 I}\right]\int_{t-T_0}^{t}R_N(t)I(t)\cos^2[\omega t+\varphi)]dt$$

Contrary to common publications, this is a time variant resistance; ideally it does not degrade the Q outside the on condition. This resistance however is “noisy”.

Since the negative resistance is related to the large signal transconductance and the feedback capacitors of the Colpitts oscillator, we can insert this in the equation above and after a lengthy set of calculation the phase noise under large signal conditions become [2, Ch-8, pp. 159-232]

$$\pounds(\omega)=10\times\log\left[\left[k_0+\left(\frac{k^3k_1\left[\frac{Y_{21}^+}{Y_{11}^+}\right]^4[y]^{4p}}{\left[Y_{21}^+\right]^6[y]^{6q}}\right)\left(\frac{1}{(y^2+k)}\right)\right]\left[\frac{[1+y]^2}{y^2}\right]\frac{Q_{\max}^2}{Q_0^2}\right] \qquad (45)$$

Where, $y=\frac{C_1}{C_2}$, $k_0=\frac{kTR}{\omega^2\omega_0^2L^2V_{cc}^2C_2^2}$, $k_1=\frac{qI_cg_m^2+\frac{K_fI_b^{AF}}{\omega}g_m^2}{\omega^2\omega_0^4L^2V_{cc}^2}$, $k_2=\omega_0^4(\beta^+)^2$, $k=\frac{k_3}{k_2C_2^2}$

This results in the phase noise values as a function of the large signal parameters. These are identified and the term k_1 adds the semiconductor noise contributions, which are now bias dependent.

The following is a first in the sense, that we calculate the exact solution of the phase noise of the transmission line, using a smaller than quarter wavelength resonator (inductive) and substitute this for the inductor. This uses a tangent function and if the losses would be applied a hyperbolic tangent function. In this case we assume that the Q is sufficiently high that the value of the $\cosh(\alpha l) \approx \sinh(\alpha l) \approx e^{\frac{\alpha l}{2}}$

The characteristic impedance of most of the coaxial resonator is approximately 10ohms and can be calculated by the following equation. D is the outer diameter or side length of the coaxial resonator, d is the inner diameter of the coaxial resonator and εr is the dielectric constant.

$$Z = \frac{60}{\sqrt{\varepsilon r}} \ln\left(\frac{D}{d}\right) = \frac{60}{\sqrt{38.6}} \ln\left(\frac{6}{2.42}\right) = 8.768\Omega$$

We know that, $L = \frac{Z_l}{\omega}$ [3]

Where, $Z_l(f) = jZ\tan(\beta l)$; $Z_l(f) = jZ\tan\left(\frac{\omega}{v_P} l\right)$;

Therefore $L = j\frac{Z}{\omega}\tan\left(\frac{\omega}{v_P} l\right)$ where, v_P is the Phase velocity and l is the length of the coaxial resonator.

As seen from this equation L is the function of frequency and needs to be calculated for each computation of frequency sweep.

So the modified equation for phase noise calculation is as follows.

$$\pounds(\omega) = 10 \times \log\left[\left[k_0 + \left(\frac{k^3 k_1 \left[\frac{Y_{21}^+}{Y_{11}^+}\right]^4 [y]^{4p}}{\left[Y_{21}^+\right]^6 [y]^{6q}}\right)\left(\frac{1}{(y^2+k)}\right)\right]\left[\frac{[1+y]^2}{y^2}\right]\right]\frac{Q_{\max}^2}{Q_0^2} \qquad (46)$$

Where, $y = \frac{C_1}{C_2}$, $k_0 = \frac{kTR}{\omega^2 \omega_0^2 \left(j\frac{Z}{\omega}\tan\left(\frac{\omega}{v_P} l\right)\right)^2 V_{cc}^2 C_2^2}$, $k_1 = \frac{qI_c g_m^2 + \frac{K_f I_b^{AF}}{\omega} g_m^2}{\omega^2 \omega_0^4 \left(j\frac{Z}{\omega}\tan\left(\frac{\omega}{v_P} l\right)\right)^2 V_{cc}^2}$, $k_2 = \omega_0^4 (\beta^+)^2$,

$k = \frac{k_3}{k_2 C_2^2}$

The phase noise equation (46) above can be differentiated to determine the best possible phase noise. This is a better approach then to depend on the optimizer of the HB simulator.

$$\frac{\partial \left| \phi^2(\omega, y, k) \right|}{\partial y} \Rightarrow 0 \qquad (47)$$

$$\frac{\partial}{\partial y}\left[\left\{\left[\left[k_0 + \left(\frac{k^3 k_1 \left[\frac{Y_{21}^+}{Y_{11}^+}\right]^4 [y]^{4p}}{\left[Y_{21}^+\right]^6 [y]^{6q}}\right)\left(\frac{1}{(y^2+k)}\right)\right]\left[\frac{[1+y]^2}{y^2}\right]\right\}\frac{Q_{max}^2}{Q_0^2}\right]_{y=m} \Rightarrow 0 \qquad (48)$$

For minimization of noise and regime of y, we leave this task and its calculation and validation to the interested reader; detailed information can be found in [2, pp. 181].

The next step is to think about improving quality factor of resonator tank circuit and techniques to minimize the phase noise for modern oscillators (narrowband and wideband voltage controlled oscillator) for current and later generation of communications systems.

Validation

Modern expensive harmonic balance based simulators such as ADS from Agilent and Serenade from Ansoft, part of Ansys, can be used to determine the resulting phase noise with a high degree of accuracy, about 2dB typical error. By introducing a novel mathematical method as shown above, based on measured large signal parameters, the correct phase noise can be calculated, relative to the simulation. Our test case is figure 12.

A similar 800MHz VCO from the standard listing of Synergy microwave was used to further validate the method. The analysis with the Harmonic balance program indicates the predicted phase noise (Figure 30). The flicker corner frequency is about 1kHz, though it is not distinctly visible due to high Q resonator in use and the the phase noise at 10 KHz offset is -132.14 dB/Hz.

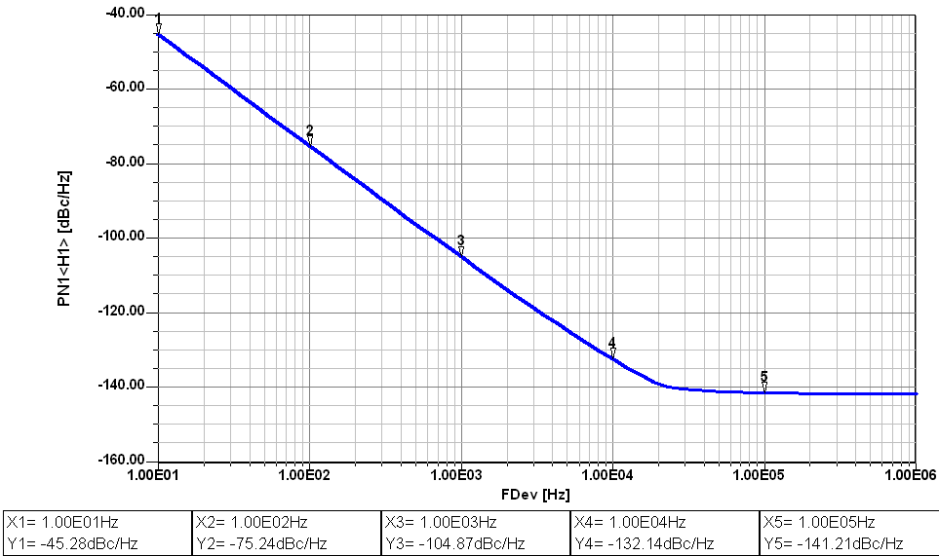

Figure 30: A CAD Simulated (Ansoft Designer) phase noise plot for 1 GHz oscillator

The simulator fails to give any change in phase noise above 1MHz offset due to numerical problems of the simulator. The calculation based on equation 46 predicted the phase noise shown in figure 31. It can show a flicker corner at 1KHz and the predicted phase noise at 10KHz is around 130.5dBc/Hz. The 10MHz offset phase noise calculates to about -170dBc/Hz.

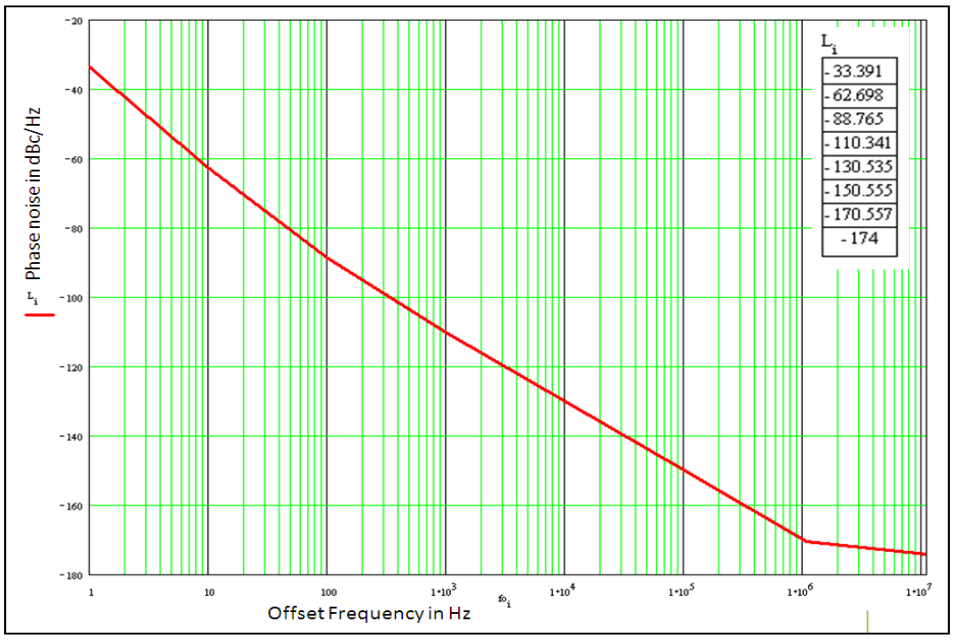

Figure 31: Predicted phase noise based on equation 46 using MathCad.

The measured response of this unit is shown verified on R&S FSUP network analyzer and the Agilent Network analyzer E5052A. Shown in Figure 32-A (R&S FSUP measurement) and Figure 32-B (Agilent E5052A measurement). This data matches well with the calculation but does not agree with the simulation at 1MHz and further out.

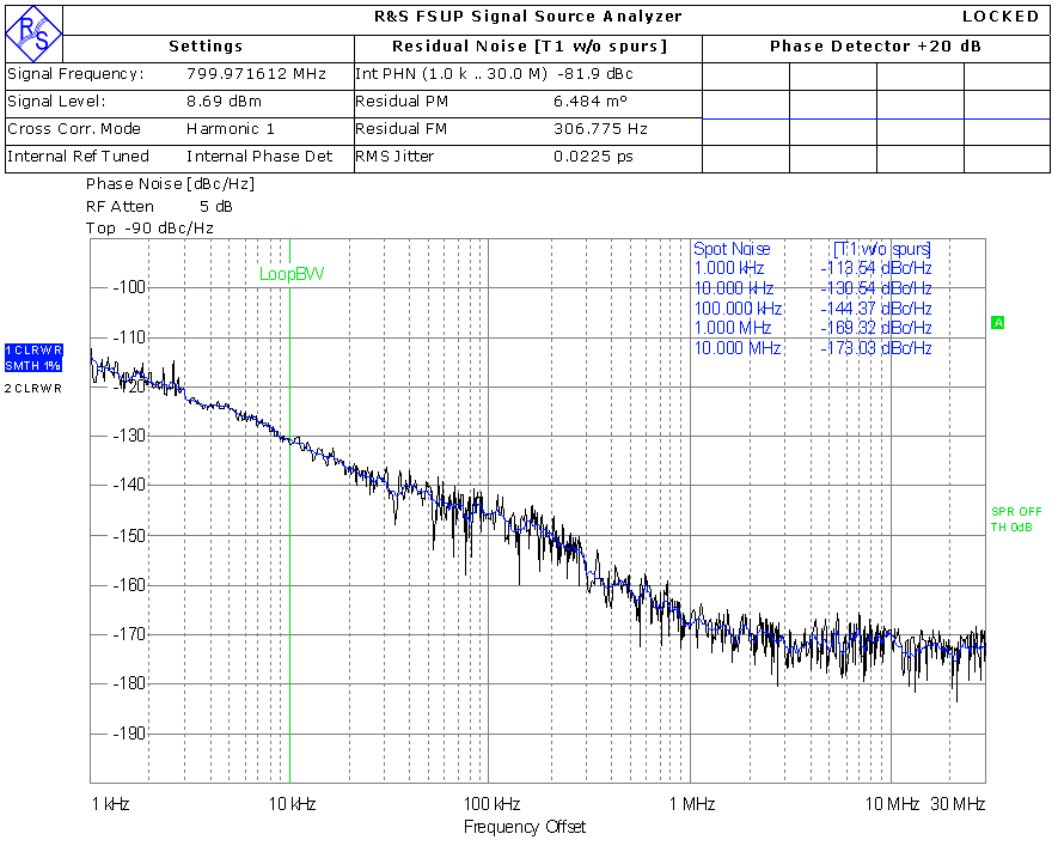

Figure 32-A: Measurement of the unit with an R&S FSUP analyzer.

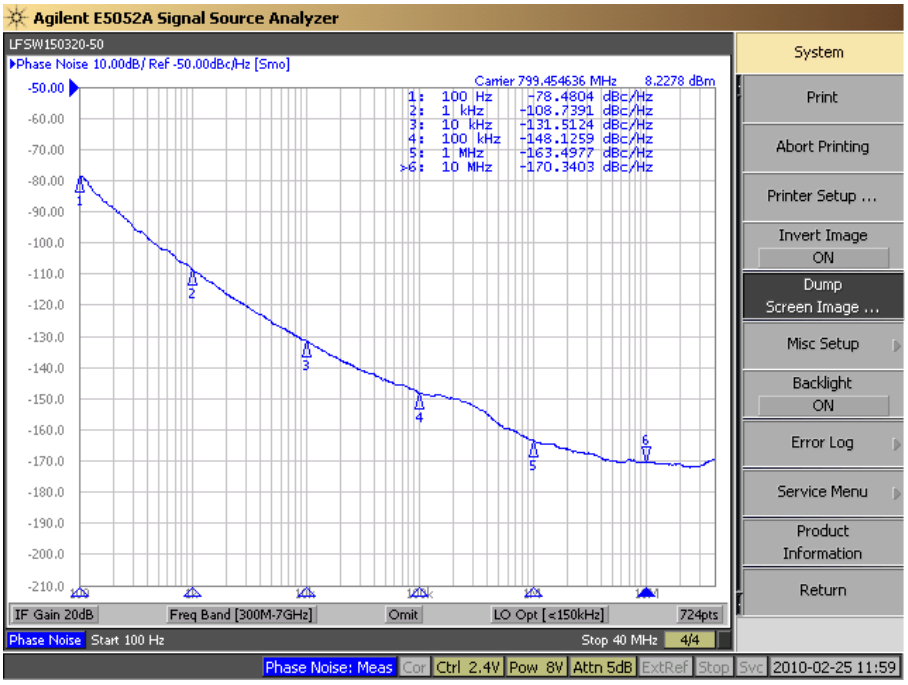

Figure 32-B: Measurement of the Unit with an Agilent E5052A analyzer.

Acknowledgements:

We would like to thank Rucha Lakhe for helping us to put this report together.

Reference:

1. Randall W. Rhea, *Discrete Oscillator Design,* Artech House, Boston, 2009.
2. U.L. Rohde, A.K. Poddar, and G. Boeck, *The Design of Modern Microwave Oscillators for Wireless Applications: Theory and Optimization*, Wiley, New York, 2005.
3. U. L. Rohde, *Transistoren bei höchsten Frequenzen,* Verlag Für Radio-Foto-Kinotechnik, Germany 1965, page 92.
4. H. Zinke and Brunswig, Volume 1 *Lehrbuch der Hochfrequenz-technik,* New York 1986 page 77.
5. G. Vendelin, A. Pavio and U. L. Rohde, *Microwave circuits design using Linear and nonlinear techniques,* Wiley, New York, 2005 page 577.
6. Michael M.Driscoll, Two-Stage Self-Limiting Series Mode Type Quartz Crystal Oscillator Exhibiting Improved Short-Term Frequency Stability, IEEE Transactions on Instrumentation and Measurement June 1973, pp130 – 138, modified by Chris Bartram, *Notes on the Driscoll VHF Overtone Crystal Oscillator and a New Low-Noise VHF Crystal Oscillator Topology* 2008.